EGYPTIAN JOURNAL OF CANCER AND BIOMEDICAL RESEARCH (EJCBR)

RESEARCH ARTICLE

Gold nanoparticles as a radio sensitizer in the treatment of triple negative breast cancer cells

Heba S. Ramadan[1], Mohaned S. Abd Elkrim[1], Bassant S. Mohamed[2,3], Tarek El-Sewedy[4]

[1]*Medical Biophysics Department, Medical Research Institute, Alexandria University, Egypt*
[2]*Basic Science Department, Faculty of Physical Therapy, Rashid University, Egypt*
[3]*Biochemistry Department, Faculty of Science, Alexandria University, Egypt*
[4]*Applied Medical Chemistry Department, Medical Research Institute, Alexandria University, Egypt*

ABSTRACT

Background: The current study intends to assess the possible impact of gold nanoparticles (AuNPs) as radiosensitizers in the treatment of breast cancer following X-ray irradiation of cell lines. AuNPs were chemically synthesized to accomplish our goal. **Materials and methods:** A transmission electron microscope was then used to evaluate the synthesised particles' physical dimensions and form. A Nano ZeTACizer particle analyser was used to measure the zeta potential of the produced solutions, and a UV-Vis spectrometer was used to record the samples' optical characteristics. The cytotoxic effects of AuNPs and X-ray irradiation on the triple negative MDA-MB-231 and ER-positive and PR-positive MCF-7 human breast cancer cell lines were evaluated using the MTT cell viability test. **Results:** According to the MTT assay, MCF-7 and MDA-MB-231 cells treated with varying concentrations of AuNps for 48 hours showed a significant dose-dependent decrease in cell viability. In terms of the cytotoxic dose required to 50% inhibit the cell proliferation process, the triple negative MDA-MB 231 cell line was more vulnerable to AuNps than the ER positive MCF-7 cells. According to our results, AuNps treatments stopped the cell cycle. This is consistent with the fact that AuNps combination treatments with X-rays produced the fewest viable cells, with necrosis accounting for up to 75% of cell death and apoptosis for the remaining 16%. All our findings point to a possible radiosensitization impact of AuNps on MDA-MB-231 cells. **Conclusion:** The radiotherapy of triple negative breast cancer cells, gold nanoparticles, as metal nanoparticles, are agents with good radiosensitizing potential.

Keywords: Breast cancer, AuNPs, X-ray, Necrosis, Radiosensitivity

Editor-in-Chief: Prof. M.L. Salem, PhD - Article DOI: 10.21608/jcbr.2025.353130.1380

ARTICLE INFO

Article history
Received: January 26, 2025
Revised: March 19, 2025
Accepted: June 23, 2025

Correspondence to
Heba Said Ramadan
Medical Biophysics Department,
Medical Research Institute,
Alexandria University, Egypt.
Email: heba.ramadan@alexu.edu.eg

INTRODUCTION

The International Agency for Research on Cancer (IARC) estimates that 21 million new instances of cancer will occur globally by 2030, making it one of the top causes of death (Siegel et al., 2020). One of the main causes of the tumor's failure to cure and later recurrence is the development of resistance to cancer treatments. Chemotherapy, surgery, and radiation therapy are the three primary therapeutic approaches used to treat cancer. High intensity ionizing radiation is precisely applied to the tumor tissue during radiotherapy, killing the tumor cells.

Radiation therapy's ability to damage healthy tissues is one of its disadvantages. Another disadvantage is that, depending on how far away they are from the radiation source, some tumor cells might receive a lower radiation dose. The cells may also develop a resistance to radiation. The sensitivity of the mitotic tumor cells is typically just marginally higher than that of the nearby healthy tissue. Therefore, the small amount of radiation needed to eliminate tumor tissue may only cause damage to normal tissue, not death.

However, the use of larger doses is required due to the development of tumor cell resistance to radiation doses, which ultimately leads to the death of healthy tissue (Merrick et al., 2021).

High-energy ionizing radiation like X-rays and gamma rays are the main ways to ionize water and/or biological components. Beams of electrons, protons, neutrons, or alpha or beta particles, along with other particle radiation types, are occasionally used to target malignant tissue. Radiation-mediated lysis results from this ionizing radiation's primary target being water. Unlike chemical lysis, this radiolysis generates free radicals like superoxide (O2-) and the hydrogen and hydroxyl radicals ($H^{\bullet}$ and $OH^{\bullet}$) as well as charged water species like H2O+ and H2O+ (Donya et al., 2014). There are still some serious issues with the treatment, even though radiation oncology has advanced significantly, leading to better radiation focus and more controlled doses. Because of

radiation resistance and the intrinsic limitations of the therapeutic system, it still necessitates a careful balancing act between its therapeutic advantages and physiological disadvantages (Kwatra et al., 2013).

The process of radiation sensitization increases the susceptibility of tumor tissues to radiation. Therefore, inert or therapeutic compounds that intensify the effects of radiation therapy are known as radio sensitizers. Interest in using formulations to enhance the effects of radiotherapy has noticeably increased recently, especially when employing metal-based nanoparticles (Gong et al., 2021).

The closely packed metal particles could selectively scatter and/or absorb high intensity gamma/X-ray radiation. This makes it possible to target biological elements within the tumor tissues with more precise and targeted destruction. They also provide an enhanced cross-section of interactions with the photons that these radiations create (Christopher Charles, 2019). The photoelectron scattering that takes place when metal surfaces are exposed to gamma radiation is another factor contributing to enhanced activity. The danger of radiation damage to healthy tissue is greatly decreased when all of these phenomena are combined to produce a lower therapeutic radiation dosage. Another name for the application of radiosensitizers composed of nanomaterials is Nanoparticle Enhanced X-ray Therapy (Kwatra et al., 2013).

Nanomedicine has become a promising field that attracts significant attention to clinical application (Kawasaki & Player, 2005). Because of their unique surface effect, distinctive size effect, and electrical and optical properties that are dependent on size and can be adjusted, AuNPs have rapidly become popular in medical applications. They are also easy to prepare, safe, and stable. In addition, it has fewer risks for diagnosis and therapy, which enables it to enter tissues more efficiently than traditional medications (Sengani et al., 2017).

Recently, Pottier et al. talked about the novel use of metals as nanoscale radio enhancers. It is feasible to use metal-based nanoscale compounds in therapeutic contexts. The metals that are most used in oncology include platinum, gold, and ruthenium. The novel pharmaceutical compounds based on metals are an alluring anticancer tactic. However, their toxicity might be the biggest disadvantage of using these medications (Pottier et al., 2014).

Kwatra et al. assessed several methods for enhancing cancer cells' radiosensitivity. The first application of nanoparticle enhanced X-ray therapy (NEXT), which uses nanoparticles as radio sensitizers, occurred in 2004. The most often used methods involve the use of metal-based NPs, nonmetal-based NPs (i.e., silicon or fullerene (C60)-based), super paramagnetic iron oxides (magnetite Fe3O4 and maghemite Fe3O4), and quantum dots (CaF, LaF, ZnS, or ZnO). Metal-/metal oxide-based nanoparticles include gold nanoparticles (GNPs), gadolinium nanoparticles, titanium nanoparticles (TiO2), silver nanoparticles (SnNPs), and hafnium nanoparticles (HfO2) (Kwatra et al., 2013). The current study aimed to examine the effectiveness and potential cytotoxicity of AuNPs as radiosensitizers against breast cancer cells (MCF-7, MDA-MB-231) following X-ray irradiation and exploring the mechanism of action.

MATERIALS AND METHODS

Synthesis of AuNPs

Twenty mL of 1.0 mM $HAuCl_4$ was brought to a rolling boil on a hot plate with stirring by a magnetic stirrer. After boiling, 2 mL of a 1% solution of trisodium citrate dihydrate ($Na_3C_6H_5O_7 \cdot 2H_2O$) was quickly added. The gold solution gradually formed as the citrate reduced gold (III). The solution was removed from heat once it turned deep red (Turkevich et al., 1951).

Characterization of AuNPs

Shape and Morphology

The physical size and shape of prepared particles was determined by transmission electron microscope, model JEM-1400 Plus electron microscope (central lab, electron microscope unit, Faculty of Science, Alex University). Using distilled water, the particle suspension was diluted by ten orders and deposited dropwise onto a 400 mesh copper grid coated with carbon film and was dried in the air until microscopic analysis.

Zeta potential

Zeta potential is a parameter that measures the electrochemical equilibrium at the particle-liquid interface. It measures the magnitude of electrostatic repulsion/attraction between particles and thus, it

has become one of the fundamental parameters known to affect stability of colloidal particles. It should be noted that that term stability, when applied to colloidal dispersions, generally means the resistance to change of the dispersion with time (Bhattacharjee, 2016). The zeta potential for prepared solution was determined by a Nano ZeTACizer particle analyzer (Malveren, UK), Central Lab, Faculty of pharmacy, University of Alexandria. Dynamic Light Scattering is used to measure particle size and molecular size. Laser Doppler Micro-electrophoresis is the technique used to measure zeta potential.

Ultraviolet-visible absorption spectroscopy (UV-Vis)

The UV-vis absorption spectra of the samples were recorded using UV-6800UV\Vis spectrometer with scanning range of 300-800 nm, Model (JENWAY – Germany).

***In Vitro* Cell Culture Study**

Cell culture

Human breast cancer (MCF-7, MDA-MB-231) cells were purchased from the Center of Excellence for Research in Regenerative Medicine and Application, Faculty of Medicine, Alexandria University. Cells were maintained in Dulbecco's modified Eagle medium (DMEM) medium (Invitrogen, Germany), supplemented with 10% Fetal bovine serum (FBS) (Invitrogen, Germany), and 1% penicillin, streptomycin (pen-strep) (Sigma-Aldrich, SA), at 37°C, 5% CO_2 in a humidified atmosphere. Adherent cells were brought into suspension by trypsinization with 0.25% trypsin/EDTA (*Invitrogen, Germany*). The MDA-MB-231 cells were divided into group 1: control cells grown without irradiation, group 2: exposed to X-ray irradiation, group 3: treated by AuNPs, and group 4: treated with AuNps and irradiated with X-ray. Experiments were performed in 3 replicas and repeated at least 3 times.

X-ray Irradiation of Breast Carcinoma

Breast Carcinoma cells were counted and seeded into 6-well plate at a density of 10^5 cells per well. The cells were then incubated under standard conditions as described above. Cells were irradiated with different doses 2, 4, 6, 8, 10 Gy of X-rays at Ayady El-Mostaqbal Oncology Hospital, Alexandria, Egypt. The experiment was repeated 3 times and the results pooled.

Both irradiated breast carcinoma cells and non-irradiated cells (control) were incubated for 72 hrs at 37°C in a humidified atmosphere with 5% CO_2. After the incubation period, cells were harvested and analyzed.

Cell Viability Assay

3-(4,5-dimethylthiazol-2-yl)-2,5 diphenyltetrazolium bromide (MTT) assay was used to determine the effects of the X-ray irradiation and AuNPs on cell proliferation. In brief, cells were irradiated with different doses of X-rays and treated with different concentration of AuNps (0.5 – 250 µg/ml) and incubated for 48 and 72 hours in 96 well plates at density of $5x10^3$ cells/well. Subsequently, 5 mg/ml of MTT was added to each well and incubated for 4 hours at 37°C. After incubation, supernatants were removed and 200 µl of dimethyl sulfoxide (DMSO) added to each well to dissolve the resultant formazan crystals. The absorbance was measured at 560 nm (A_{570}) using the Glomax multidetection system. The half maximal inhibitory concentration (IC_{50}) is a quantitative measure that indicates how much AuNps is needed to inhibit cancer cell proliferation by 50% of the control level. The IC_{50} for AuNps were determined from regression analysis of sigmoidal dose-response curves. (Petushkov et al., 2010).

Clonogenic Assay

The clonogenic assay was used to assess the colony-forming capacity of treated cells. In brief, 6,000 cells/ well MDA-MB-231 cells were plated in 12-well plate. The cells were allowed to adhere for 24 h before being subjected to single treatment or in combination as described above. After 48hrs, the medium was removed and replaced with fresh culture medium. The cells were incubated for 14 days, and the medium was changing twice a week. At the end of 14-day period, the medium was removed and the colonies were washed with PBS twice and fixed with absolute methanol for 20 minutes. The methanol was then removed, and 0.5% crystal violet was added to each well for 3 min. Subsequently, the colonies were washed with PBS and left for drying at room temperature (Franken et al., 2006).

Assessment of cell death mechanism by flow cytometry

MDA-MB-231 cells (1×10^6 cell/well) were seeded in 6-well plate. After 24 hours, the supernatant was aspirated, and cells were treated as described above. After the incubation period, the cells were trypsinized and centrifuged at 3,000 rpm for 5 minutes, and subsequently, the Annexin V-FITC apoptosis detection kit (Sigma-Aldrich, 640914) was employed according to the manufacturer's instructions. Cells were suspended in binding buffer and stained using 5µl FITC Annexin V and 10µl PI solution. The staining process involved gentle vortexing at 25 °C for 15 minutes in darkness. Finally, samples were analyzed with the Becton Dickinson FACS-Calibur flow-cytometer using CellQuest Pro Software for data acquisitioning. The negative control contained unstained cells. Based on the fluorescence intensity of Annexin V-FITC and PI, the populations were sorted into four categories as follows: cells negative for both Annexin V-FITC and PI in the lower left quadrant (depicting normal viable cells); cells positive for Annexin-V but negative for PI in the lower right quadrant (indicating early apoptotic cells); cells positive for both Annexin-V and PI in the upper right quadrant (representing late apoptotic cells); and cells positive for PI but negative for Annexin V-FITC in the upper left quadrant (indicating necrotic cells) (Somaida et al., 2020)

Assessing Cell Cycle Status via Flow Cytometry

In a 6 well plate, $1x10^6$ MDA-MB-231 cells were treated according to their allocated groups. Following the incubation period, the cells were harvested, centrifuged, washed with ice cold PBS and fixed by ice-cold 70% ethanol slowly at 4ºC for 30 min. The cells were suspended in 200 µg/ml DNase-free RNase A before being stained with 50 µg/ml propidium iodide (PI). Cells were analyzed by Flow Cytometry using the Cellquest Pro version 5.2.1 software to determine the percentage of cells in each phase of the cell cycle (Kim & Sederstrom, 2015)

Statistical Analysis

Statistical differences between treatments and controls were calculated using the SPSS software by one-way ANOVA followed by Tukey-Kramer Multiple comparison test. The data were expressed as mean ± standard Error of mean (SEM) of three independent experiments. *P value ≤ 0.05, **P ≤ 0.01 and ***P ≤ 0.001 were considered significant

RESULTS

Characterization of citrate coated gold nanoparticles

Shape and Morphology:

The transmission electron microscope (TEM) was used to look at the prepared particles' form. The produced citrate gold particles are entirely spherical in shape, have a smooth surface, and range in size from 11.44 to 24.57 nm, with a mean size of 15.97 ± 2.18 nm (Figure 1a).

Nano Zeta particle analyzer

To calculate the surface charge of nanoparticles in solution, the zeta potential of prepared particles was calculated. Citrate-coated AuNPs had a zeta potential of - 46.7 mV and a conductivity of 0.965 mS/cm, as illustrated in Figure 1b.

Ultraviolet-visible absorption spectroscopy (UV-Vis)

The UV-Vis spectrophotometer was used to measure the absorbance of the spectra of generated particles. According to Figure 1c, the absorbance of the gold NPs was visible and reached its greatest peak at 520 nm.

***In Vitro* Studies**

Effect of X-ray on the Viability of MCF-7 and MDA-MB-231 Cells

As shown in Figure 2 A, irradiation of MCF-7 cells caused a significant (P ≤0.05) dose and time-dependent reduction in MCF-7 cell viability compared to the control group (0 Gy). The TNBC cell line, MDA-MB-231 cells statistically responded to X-ray irradiation similarly to MCF-7 (P ≤0.05), but to a relatively lower extent, also reducing the cell viability in a dose and time-dependent manner (Figure. 2 B).

Collectively, data showed that following exposure to X-rays, the relative survival rate for MCF-7 and MDA-MB-231 cells declined in a time- and dose-dependent manner, with MDA-MB-231 showing a higher survival rate compared to that of MCF-7 cells.

AuNps Impact on MCF-7 and MDA-MB 231 Cell Viability

MTT assays disclosed that treating MCF-7 cells with different concentrations of AuNps for 48 hrs resulted in dose-dependent gradual significant reduction in

MCF-7 cell viability (P ≤0.05) compared to control; starting at a concentration of 2 µM, with a calculated

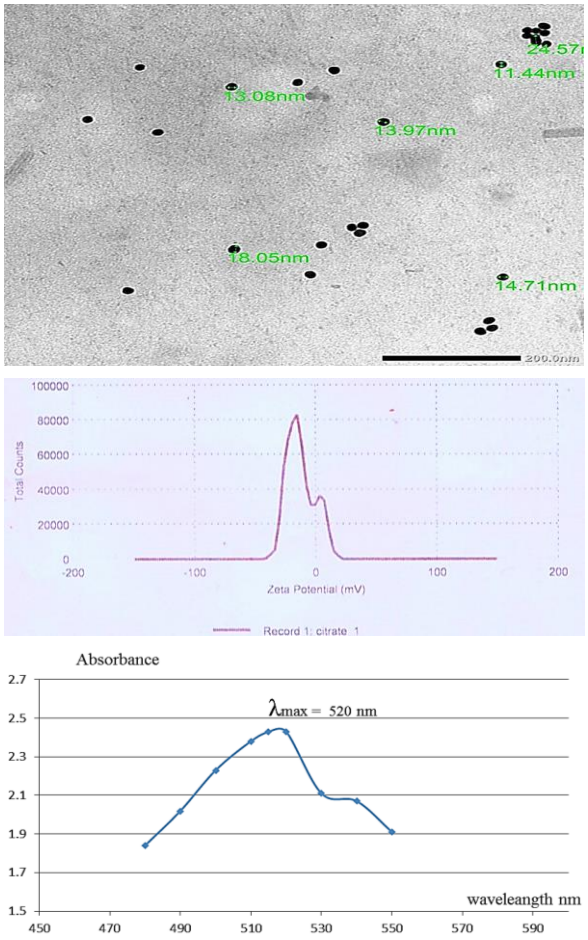

Figure 1. A) Representative images by transmission electron microscope (TEM) showing the Citrate-coated AuNPs, B) Zeta distribution for citrate coated AuNPs, C) Absorbance of citrate coated nanoparticles.

IC_{50} of AuNps at 10 ±2.12 µM that indicate a 50% reduction in cell proliferation (Figure 3 A). On the other hand, and opposite to what was observed after X-ray treatment, and MCF-7 cells, MDA-MB 231 cells were more sensitive towards AuNPs treatment, starting a significant reduction (P ≤0.05) in cell viability at only 1.0 µM AuNPs, with an observed lower IC_{50} value of 7.8 ±1.39 µM as shown in Figure 3 B.

Long Term Impact of Different Treatments on Colony Formation

As presented in Figure 4, the control group exhibited well-defined numerous colonies, whereas all treatment modalities displayed a complete loss of colonies as no colony were observed in any of the treatments compared to control. This observation underscores the potent anti-clonogenic potential of AuNPs, X-ray radiation, and their combined treatment in inhibiting cancer cell proliferation.

Effect of AuNPs and X-rays on Cell Death Mechanism (Apoptosis vs. Necrosis)

As shown in Figure 5, the control untreated cells had the highest percentage of viable cells (94.84±0.54) while combined treatment resulted in the lowest percentage of viable cells (8.79±0.29). X-ray treatment significantly reduced viability and increases early apoptosis, late apoptosis, and necrosis compared to control cells. The significant highest percentage of early apoptotic cells was detected in X-ray treated group (15.67±0.71) followed by AuNps treated group (3.65±0.34). AuNps treatment reduces viability and affects early and late apoptosis as well as necrosis but not as strongly as X-ray. All treatment groups caused a significant increase in cell populations undergoing late apoptosis. However, the highest percentage of late apoptotic cells was detected in combined treatment (15.72±0.3). Similarly to what was observed in the late apoptosis populations, the largest population of necrotic cells was detected in combined treatment group (75.22±0.1) which was significantly higher than single treated X-ray (26.46±0.54) and AuNps (24.91±0.74). Overall, combined treatment significantly induced apoptosis and necrosis in MDA-MB-231 cells showing the most potent effects compared to single treatments.

Impact of Treatments on Cell Size and Granularity of MDA-MB-231

Data in Figure 6 reveals that the control group showed a significant uniformed small size, and low complexity or granularity. The X-ray treated group is like control, but with a slight increase in the spread towards SSC which indicates that X-ray causes a minimal increase in intracellular granularity. Treatment of MDA-MB-231 with AuNps caused a noticeable dispersed population of cells with a significant increase in intracellular granularity and cell size, revealing significant increases in both cell size and complexity. Combination treatment caused the greatest alterations in cellular characteristics. This may imply a synergistic impact, which augments cellular responses like autophagy or apoptosis.

Efficacy of Combined Treatment on Cell Cycle Distribution Analysis

As shown in Figure 7, following treatment with AuNPs, there was a slightly increase in the fraction of cells in G0/G1 (66.88±0.26) and S phase (13.01±0.31)

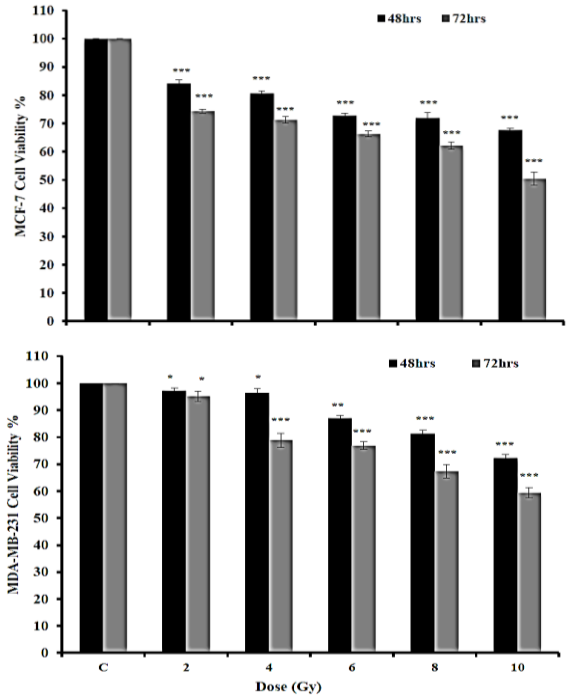

Figure 2. *In vitro* cell viability of A) MCF-7 cells against X-ray, using different doses for 48hrs and 72 hrs. B) MDA-MB-231 cells against X-ray, using different doses for 48hrs and 72 hrs. Each data point is an average of three independent experiments and expressed as Mean ±SEM.

with a concomitant decrease in the fraction of cells in the G2/M phase (8.97±0.77) compared to control group that represents 61.17±1.11, 10.46±0.36 & 14.28±0.59 respectively in G0/G1, S & G2/M phases. This indicates AuNPs were able to arrest cell cycle at G0/G1 phase and therefore accumulate cells.

The most dramatic G2/M cell cycle arrest (30.10±0.26) was caused by combined treatment with a significant reduction in G0/G1 phase cells (42.49±0.62) relative to control cells. It also demonstrates a significant difference compared to X-ray alone in the G2/M phase (21.43±1.4), indicating a potential synergistic effect of the combined treatment. These findings suggest that although both AuNPs and X-ray individual treatments affect the distribution of the cell cycle, their combination produces more pronounced alterations, especially an increase in the G2/M phase, suggesting the possibility of enhanced cell cycle arrest when combined.

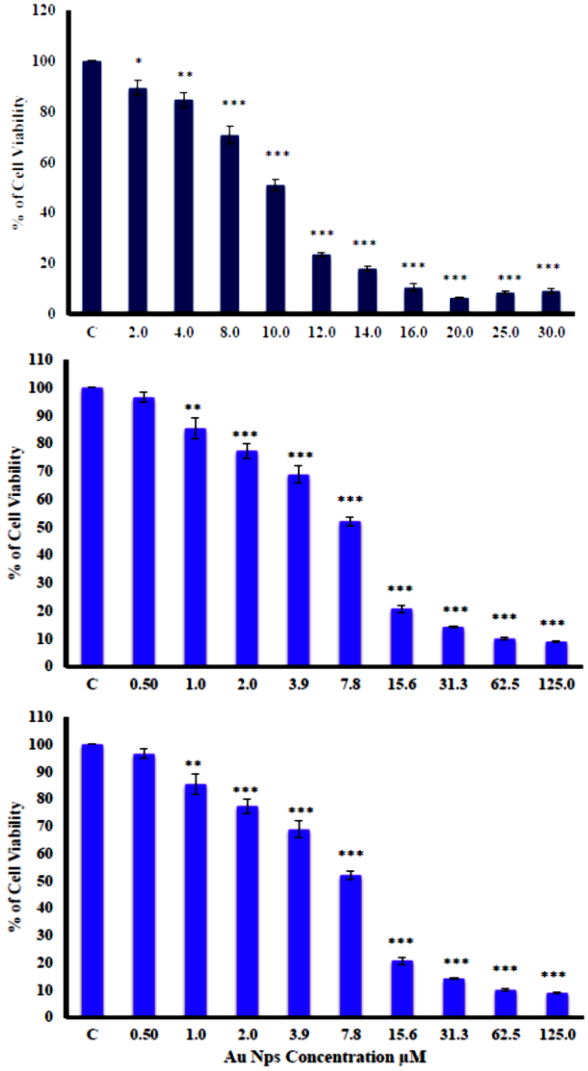

Figure 3. *In vitro* cell viability of A) MCF-7 cells against AuNps, using different doses for 48hrs. B) MDA-MB-231 cells against AuNps, using different doses for 48hrs. Each data point is an average of three independent experiments and expressed as Mean ±SEM.

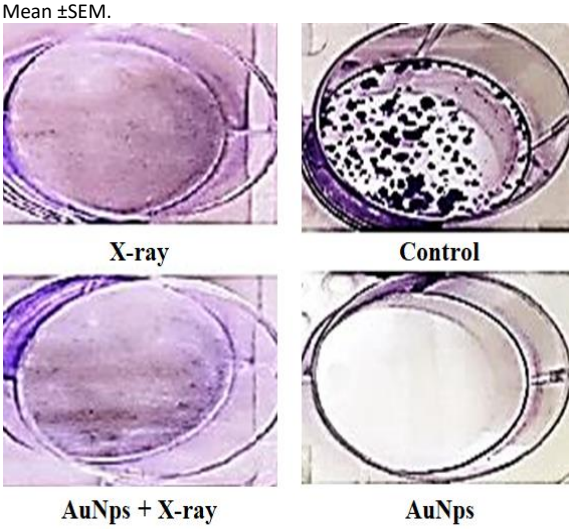

Figure 4. Effect of AuNP, X-ray & their combined treatments on colony formation of MDA-MB-231 cells. Analysis of clonogenic assay revealed a significant reduction in colony formation, indicating the potent anti-clonogenic effects of the treatments.

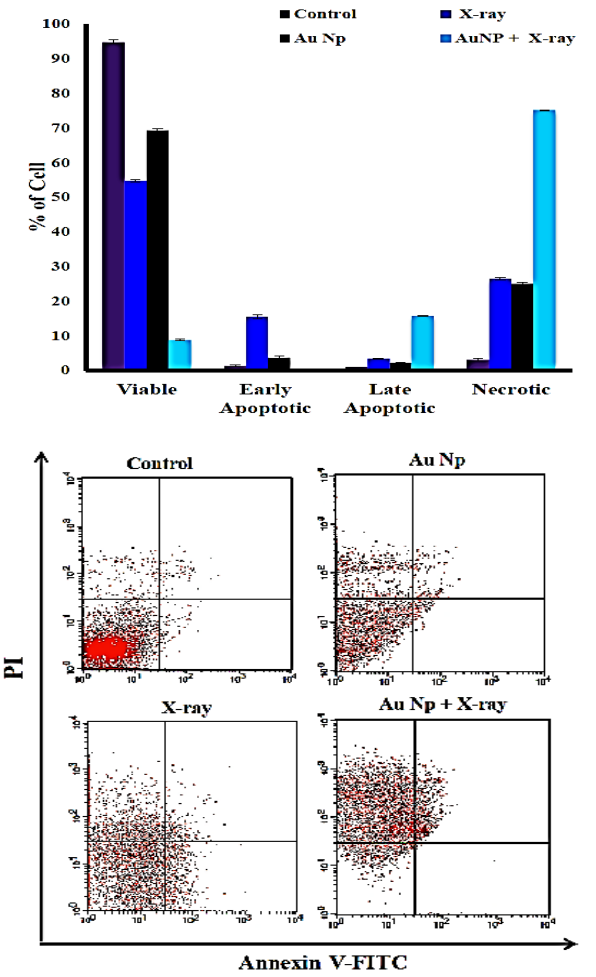

Figure 5. Evaluation of molecular mechanism of cell death in MDA-MB-231 cells: **(A)** Bar chart showing the percentage of viable, early apoptotic, late apoptotic and necrotic MDA-MB-231 cell populations after different treatments. **(B)** Representative dot plots images showing the cell population of each quadrant.

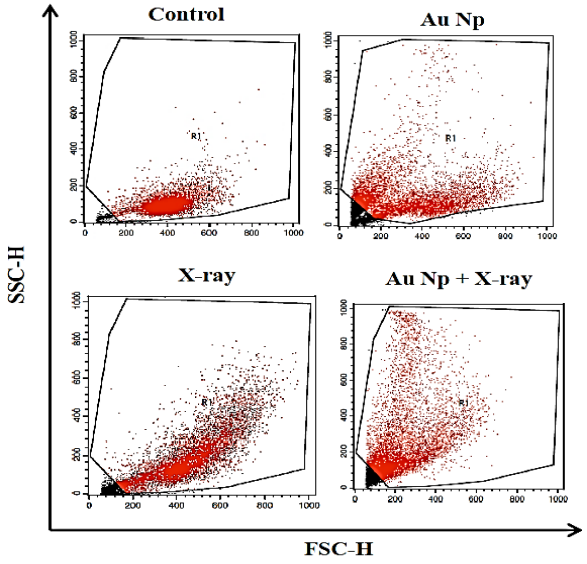

Figure 6. Representative dot plots showing dot plots for forward (FSC-H) and side scatter (SSC-H) flow cytometry analysis for MDA-MB-231 cells after treatment.

DISCUSSION

The simplicity and adaptability of gold nanoparticles synthesis techniques have drawn a lot of interest in gold nanoparticles (AuNPs) for use in medicine. This allows for the creation of a range of sizes and shapes with various surface coatings to optimize their therapeutic efficacy (Sztandera et al., 2018). In this work, we presented a thorough analysis of the characterization and therapeutic potential of citrate-coated AuNPs against triple negative MDA-MB-231 and MCF-7 cell lines, both by themselves and in combination with X-ray irradiation. Triple negative breast cancer has numerous subgroups based on genetic, pathologic, and clinical characteristics, according to Tomao F et al. Thus, the development of novel, molecularly focused treatments would be highly advantageous for patients with TNBC, a biologically aggressive cancer (Tomao F et al., 2015).

The cytotoxic effects of AuNPs and X-ray irradiation on MDA-MB-231 and MCF-7 breast cancer cell lines were evaluated using the MTT test. Following treatment with varying dosages of AuNps, the viability of MCF-7 and MDA-MB-231 cells dramatically decreased in a dose-dependent manner. Remarkably, MDA-MB-231 cells had an IC50 value of 10±2.12 µM, indicating a greater sensitivity to AuNPs.

The two cell lines' low IC50 values for AuNps contrast with the high cytotoxic dose needed in a prior study by Balakrishnan et al., who found no discernible cytotoxicity at lower doses other than when using extremely high doses for both cell lines (up to 100 and 125 µM, respectively) (Balakrishnan et al., 2016). This suggests that our synthesized AuNPs were remarkably effective as a cytotoxic compound with superior quality and internalization efficiency.

Additionally, X-ray irradiation reduced cell survival in a time and dosage dependent manner, with MCF-7 cells showing a more noticeable effect. This is consistent with Wang et al.'s findings showing, when compared to the sham-irradiated control group, high dosage X-ray irradiation greatly suppressed the development of MCF-7 cells in a dose-dependent manner, with the 10 Gy irradiation having the most significant effect (Wang et al., 2018). Our research showed that MDA-MB-231 cells were more vulnerable to the synthesised AuNps, even though they are thought to be less radiosensitive and more

aggressive than MCF-7 cells because of their triple negative condition (Zhang and others, 2020) According to other research, MDA-MB 231 cells responded better to anticancer medications than MCF-7 cells (Bettelli et al., 2006; Jokar et al., 2019).

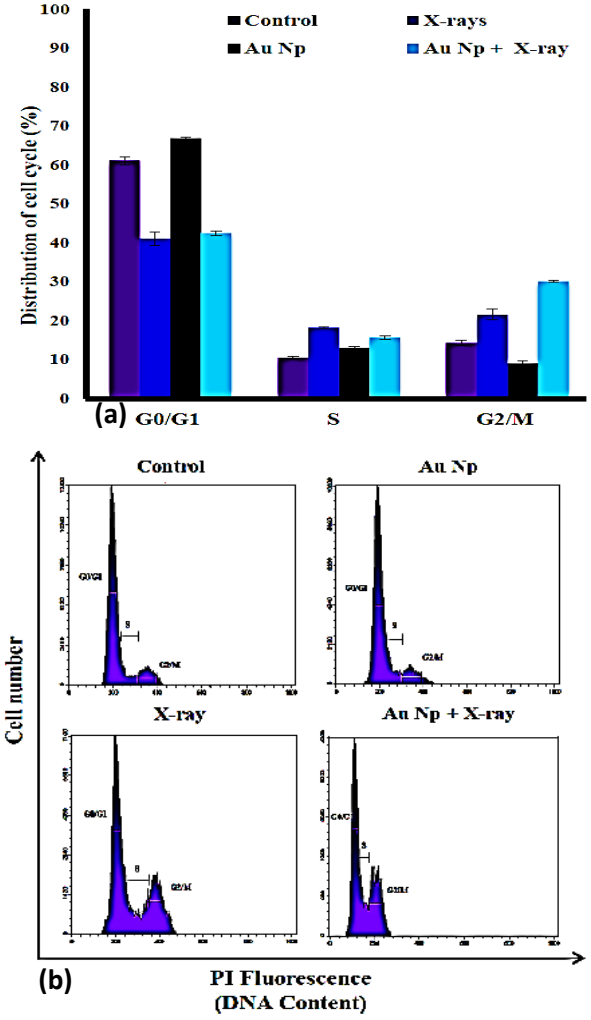

Figure 7. A) Cell Cycle distribution percentage of control and treated MDA-MB-231 cells demonstrating of cell % in G0/G1, S and G2/M cell cycle phases. B) Flow cytometry analysis histogram of cell cycle parameters.

Our study examined the possible long-term effects of AuNPs, X-rays, and their combined therapy on MDA-MB-231 cells. The substantial reduction in MDA-MB-231 colony formation following treatment suggests that these therapies have robust anti-clonogenic properties. Human colorectal cancer, MDA-MB-231, and several other cell lines demonstrated highly significant and dose-dependent suppression of colony formation by X-ray irradiation, which is consistent with our findings (Veldwijk et al., 2014; Malyarenko et al., 2020) In the same manner, AuNPs also inhibited colony formation of pancreatic cancer cells and MCF-7 breast cancer cells (Huai et al., 2019; Singh et al., 2021). We have investigated the potential mechanism leading for such cytotoxicity in MDA-MB-231 cells by detecting the cell cycle status and apoptosis using flow cytometry (Sica et al., 2016).

The results of Annexin V-FITC/PI staining revealed that necrosis was the main cause of cell death (up to 75%) when compared to single treatments, with apoptosis coming in second (16%). The combination treatment increases the induction of cell death pathways, resulting in a more effective therapeutic strategy. Notably, necrotic cells developed throughout the X-ray treatment, suggesting that radiation-exposed cells transitioned from apoptosis to necrosis. These results imply that necrosis, rather than apoptosis, was the primary cause of cell death following combination treatment; this discovery may be important for cancer cells that are resistant to apoptosis and have defects in some part of the apoptotic machinery. Necroptosis, also known as programmed necrosis, is therefore being considered as a possible substitute anticancer tactic (Cho & Park, 2014). Necrosis and apoptosis have been observed concurrently in various human diseases, suggesting that they are connected processes rather than completely distinct ones. These findings support previous studies that demonstrated AuNPs produce necroptosis in lung cancer and leukemic cells, indicating that necrosis is a key mechanism of AuNP-induced cell death (Liu, M. et al., 2013, Martinez-Torres et al., 2019)

Furthermore, one of the primary morphological changes that are frequently connected to necrosis is cell swelling, which causes the cells to enlarge. Physiological processes like senescence and autophagy, which are essential for the effectiveness of cancer chemotherapies, coincide with increases in intracellular granularity, making them a helpful indicator to screen for new cancer treatment drugs (Haynes et al., 2009). The greatest increase in cell size and granularity was observed with the combined therapy. This increase raises the possibility that autophagic or cell death pathways have been activated. This result is in line with the combined therapy group's increased rate of cell death, suggesting that the combination results in more pronounced cellular reactions. Our findings are consistent with previous in vitro research that showed AuNp's capacity to trigger autophagy

through the accumulation of autophagosomes (Ma et al., 2011; Chen et al., 2020; Guo et al., 2020). Cell death is made possible by the concentration of cells in the G2/M phase during arrest, and this could be a useful tactic in cancer treatment (Montenegro et al., 2015). The highest G2/M phase arrest was considerably produced by the combination treatment, suggesting a disruption in the cycle progression that could lead to reduced cell proliferation and increased sensitivity to therapeutic interventions. Additional support for the potential synergy between AuNPs and X-ray irradiation is provided by the notable effect on the G2/M phase when compared to separate treatments.

CONCLUSION

The current study showed that when applied to triple negative breast cancer cells, citrate-coated gold nanoparticles have a high radiosensitizing capacity in cancer radiation therapy. These nanoparticles have strong anti-cancer effects thanks to their promotion of necrosis, apoptosis, and cell cycle arrest. High Z coefficient, biocompatibility, and simplicity of manufacturing and modification are only a few of the beneficial physicochemical properties of gold nanoparticles. Future research must concentrate on molecular knowledge and in vivo validation to enhance these therapy modalities and possible side effects.

AUTHORS' CONTRIBUTION

All authors have participated in the concept and design, analysis and interpretation of data, revision of the manuscript and they have approved the manuscript as submitted.

CONFLICT OF INTEREST

None

FUNDING

None

REFERENCES

Balakrishnan, S., Bhat, F. A., Raja Singh, P., Mukherjee, S., Elumalai, P., Das, S. & Arunakaran, J. (2016). Gold nanoparticle-conjugated quercetin inhibits epithelial-mesenchymal transition, angiogenesis and invasiveness via EGFR/VEGFR-2-mediated pathway in breast cancer. *Cell proliferation,* 49(6), 678-697.

Bettelli, E., Carrier, Y., Gao, W., Korn, T., Strom, T. B., Oukka, M. & Kuchroo, V. K. (2006). Reciprocal developmental pathways for the generation of pathogenic effector TH17 and regulatory T cells. *Nature,* 441(7090), 235-238.

Bhattacharjee, S. (2016). DLS and zeta potential – What they are and what they are not? *Journal of Controlled Release, 235*, 337-351.

Chen, R. J., Chen, Y. Y., Liao, M. Y., Lee, Y. H., Chen, Z. Y., Yan, S. J. & Wang, Y. J. (2020). The Current Understanding of Autophagy in Nanomaterial Toxicity and Its Implementation in Safety Assessment-Related Alternative Testing Strategies. *International Journal of Molecular Sciences, 21*(7).

Cho, Y. S., & Park, S. Y. (2014). Harnessing of Programmed Necrosis for Fighting against Cancers. *Biomolecules & therapeutics, 22*(3), 167-175.

Christopher Charles, B. (2019). *The Secondary Photoelectron Effect: Gamma Ray Ionisation Enhancement in Tissues from High Atomic Number Elements*. China: Intechopen.

Colturato-Kido, C., Lopes, R. M., Medeiros, H. C. D., Costa, C. A., Prado-Souza, L. F. L., Ferraz, L. S., & Rodrigues, T. (2021). Inhibition of Autophagy Enhances the Antitumor Effect of Thioridazine in Acute Lymphoblastic Leukemia Cells. *Life,* 11(4), 365.

Donya, M., Radford, M., ElGuindy, A., Firmin, D., & Yacoub, M. H. (2014). Radiation in medicine: Origins, risks and aspirations. *Global cardiology science & practice,* 4, 437-448.

Franken, N. A., Rodermond, H. M., Stap, J., Haveman, J., & van Bree, C. (2006). Clonogenic assay of cells in vitro. *Nature protocols, 1*(5), 2315-2319.

Gong, L., Zhang, Y., Liu, C., Zhang, M., & Han, S. (2021). Application of Radiosensitizers in Cancer Radiotherapy. *International journal of nanomedicine, 16*, 1083-1102.

Guo, L., He, N., Zhao, Y., Liu, T., & Deng, Y. (2020). Autophagy Modulated by Inorganic Nanomaterials. *Theranostics, 10*(7), 3206-3222.

Haynes, M. K., Strouse, J. J., Waller, A., Leitao, A., Curpan, R. F., Bologa, C. & Thompson, T. A. (2009). Detection of intracellular granularity induction in prostate cancer cell lines by small molecules using the HyperCyt high-throughput flow cytometry system. *Journal of biomolecular screening, 14*(6), 596-609.

Huai, Y., Zhang, Y., Xiong, X., Das, S., Bhattacharya, R., & Mukherjee, P. (2019). Gold Nanoparticles sensitize pancreatic cancer cells to gemcitabine. *Cell stress, 3*(8), 267-279.

Jokar, F., Mahabadi, J. A., Salimian, M., Taherian, A., Hayat, S. M. G., Sahebkar, A., & Atlasi, M. A. (2019). Differential Expression of HSP90β in MDA-MB-231 and MCF-7 Cell Lines after Treatment with Doxorubicin. *Journal of pharmacopuncture,* 22(1), 28-34.

Kawasaki, E., & Player, A. (2005). Nanotechnology, nanomedicine, and the development of new, effective therapies for cancer. *Nanomedicine, 1*, 101-109.

Kim, K. H., & Sederstrom, J. M. (2015). Assaying Cell Cycle Status Using Flow Cytometry. *Current protocols in molecular biology, 111*, 1-11.

Kwatra, D., Venugopal, A., & Anant, S. (2013). Nanoparticles in radiation therapy: a summary of various approaches to enhance radiosensitization in cancer. *Translational Cancer Research, 2*(4), 330-342.

Liu, M., Gu, X., Zhang, K. et al. (2013). Gold nanoparticles trigger apoptosis and necrosis in lung cancer cells with low intracellular glutathione. *J Nanopart Res.*, 15: 1745

Ma, X., Wu, Y., Jin, S., Tian, Y., Zhang, X., Zhao, Y. & Liang, X. J. (2011). Gold nanoparticles induce autophagosome accumulation through size-dependent nanoparticle uptake and lysosome impairment. *ACS nano, 5*(11), 8629-8639.

Malyarenko, O. S., Imbs, T. I., & Ermakova, S. P. (2020). In Vitro Anticancer and Radiosensitizing Activities of Phlorethols from the Brown Alga Costaria costata. *Molecules,* 25(14).

Martinez-Torres AC, Lorenzo-Anota HY, García-Juárez MG, Zarate-Triviño DG, Rodríguez-Padilla C. (2019). Chitosan gold nanoparticles induce different ROS-dependent cell death modalities in leukemic cells. *Int J Nanomedicine*, 14: 7173-7190.

Merrick, M., Mimlitz, M. J., Weeder, C., Akhter, H., Bray, A., Walther, A. & Ekpenyong, A. (2021). In vitro radiotherapy and chemotherapy alter migration of brain cancer cells before cell death. *Biochemistry and Biophysics Reports, 27*, 101071.

Montenegro, M. F., Sánchez-del-Campo, L., Fernández-Pérez, M. P., Sáez-Ayala, M., Cabezas-Herrera, J., & Rodríguez-López, J. N. (2015). Targeting the epigenetic machinery of cancer cells. *Oncogene, 34*(2), 135-143.

Petushkov, A., Ndiege, N., Salem, A. K., & Larsen, S. C. (2010). Toxicity of Silica Nanomaterials: Zeolites, Mesoporous Silica, and Amorphous Silica Nanoparticles. In J. C. Fishbein (Ed.), *Advances in Molecular Toxicology* (p.p. 223-226). London: Elsevier.

Pottier, A., Borghi, E., & Levy, L. (2014). New Use of Metals as Nanosized Radioenhancers. *Anticancer research, 34*, 443-453.

Sengani, M., Grumezescu, A., & Rajeswari, D. (2017). Recent trends and methodologies in gold nanoparticle synthesis – A prospective review on drug delivery aspect. *OpenNano, 2*, 37-46.

Sica, V., Maiuri, M. C., Kroemer, G., & Galluzzi, L. (2016). Detection of apoptotic versus autophagic cell death by flow cytometry. *Programmed Cell Death* (1-16). New York, NY: Humana Press.

Siegel, R. L., Miller, K. D., & Jemal, A. (2020). Cancer statistics, 2020. *CA: A Cancer Journal for Clinicians, 70*(1), 7-30.

Singh, N., Das, M. K., Ansari, A., Mohanta, D., & Rajamani, P. (2021). Biogenic nanosized gold particles: Physico-chemical characterization and its anticancer response against breast cancer. *Biotechnology reports (Amsterdam, Netherlands), 30*, e00612.

Somaida, A., Tariq, I., Ambreen, G., Abdelsalam, A. M., Ayoub, A. M., Wojcik, M. & Bakowsky, U. (2020). Potent Cytotoxicity of Four Cameroonian Plant Extracts on Different Cancer Cell Lines. *Pharmaceuticals, 13*(11), 357.

Sztandera, K., Gorzkiewicz, M., & Klajnert-Maculewicz, B. (2018). Gold nanoparticles in cancer treatment. *Molecular pharmaceutics, 16*(1), 1-23.

Tomao F, Papa A, Zaccarelli E, Rossi L, Caruso D, Minozzi M, Vici P, Frati L and Tomao S. (2015) Triple-Negative Breast Cancer: New Perspectives for Targeted Therapies. *Onco Targets Ther* 8: 177-193.

Turkevich, J., Stevenson, P. C., & Hillier, J. (1951). A study of the nucleation and growth processes in the synthesis of colloidal gold. *Discussions of the Faraday Society, 11*(1), 55-75.

Veldwijk, M. R., Zhang, B., Wenz, F., & Herskind, C. (2014). The biological effect of large single doses: a possible role for non-targeted effects in cell inactivation. *PloS one,* 9(1), e84991.

Wang, Z. F., Sun, W. Y., Yu, D. H., Zhao, Y., Xu, H. M., He, Y. F., & Li, H. J. (2018). Rotundic acid enhances the impact of radiological toxicity on MCF-7 cells through the ATM/p53 pathway. *International journal of oncology, 53*(5), 2269-2277.

Zhang, Q., Kong, Y., Yang, Z., Liu, Y., Liu, R., Geng, Y., Luo, H., Zhang, H., Li, H., Feng, S., & Wang, X. (2020). Preliminary study on radiosensitivity to carbon ions in human breast cancer. *Journal of Radiation Research*, 61(3): 399-409.